Effect of Concrete Thickness and Expanded Polystyrene Layer on Stiffness and Floor Impact Sound Insulation Performance of Cross-Laminated Timber Slabs

Sung-Jun Pang [a], Hyo-Jin Lee [b], Yeon-Su Ha [c], Chul-Ki Kim [d], Ji-Ho Chang [e], Ho-Jeong Cho [a], and Sang-Joon Lee [d,*]

Effects of an expanded polystyrene (EPS) layer and varying precast concrete thickness were investigated relative to the stiffness and acoustic performance of cross-laminated timber (CLT) slabs. Six different concrete thicknesses and EPS layers were applied to larch and pine CLT slabs for testing. Airborne sound transmission loss (D_w) was measured using speakers, light impact sound ($L_{nT,w}$) using a tapping machine, and heavy impact sound ($L_{iA,Fmax}$) using rubber balls, in accordance with KS F ISO717-2. The results indicated that the EPS layer significantly improved light impact sound insulation (by 8 dB) and airborne noise insulation (by 5 dB), but had a minimal effect on heavy impact sound (0.5 dB). Both stiffness and sound insulation increased with concrete thickness, although improvement plateaued beyond 100 mm for larch CLT and 150 mm for pine CLT. The flexural and impact stiffness of larch CLT slabs were 24.3% and 19.2% higher than those of pine CLT slabs, respectively. Moreover, impact stiffness had a stronger correlation with acoustic performance than the previously established relationship with area density.

DOI: 10.15376/biores.21.1.2101-2122

Keywords: Cross-laminated timber; Expanded polystyrene; Floor impact sound; Airborne sound; Stiffness

*Contact information: a: Department of Wood Science and Engineering, Chonnam National University, Gwangju, Republic of Korea; b: Fire Insurers Laboratories of Korea, Yeoju-si, Republic of Korea; c: Korea Institute of Civil Engineering and Building Technology, Goyang-si, Republic of Korea; d: National Institute of Forest Science, Seoul, Republic of Korea; e: VizWave Inc., Seongnam-si, Gyeonggi-do, Republic of Korea; *Corresponding author: lsjoon@korea.kr*

INTRODUCTION

Timber, a renewable construction material, can store carbon, and the Intergovernmental Panel on Climate Change (IPCC) recognizes it as an effective carbon sink (Arehart *et al.* 2021; Bjånesøy *et al.* 2023). According to the IPCC guidelines (Penman *et al.* 2006), harvested wood products produced and used within a country can play a crucial role in delaying carbon emissions. These products can store carbon for extended periods, particularly when used in construction, where they may retain carbon for over 80 years (Lippke *et al.* 2010). Moreover, even after their service life, wood products can continue to offset emissions through recycling and energy recovery (Pajchrowski *et al.* 2014; Berger *et al.* 2020; Kromoser *et al.* 2022). Consequently, using timber in construction not only reduces carbon emissions but also contributes to global climate change mitigation.

Cross-laminated timber (CLT) has emerged as a leading mass timber product in the construction industry, offering significant advantages, including improved structural stability and efficient prefabrication (Harte 2017; Loss *et al.* 2016a,b). With active research and industrial application in Europe and North America, CLT has been widely used in

high-rise residential buildings. In Korea, CLT manufacturing methods were standardized in 2021 (Eom *et al.* 2019; KS F 2081 2021; Lee *et al.* 2023), raising expectations for broader use in the construction sector and creating opportunities for innovation and sustainable building practices that support carbon neutrality and efficient forest resource utilization (Ha *et al.* 2023).

One of the major challenges in high-rise apartments is inter-floor noise, which is particularly problematic in densely populated urban areas (Gibson *et al.* 2022; Kang *et al.* 2023). South Korea enforces some of the strictest inter-floor noise regulations globally, requiring impact sound levels in apartment buildings with over 30 units to remain below 49 dB (Ministry of Land, Infrastructure and Transport 2022). For timber residential buildings to gain wider acceptance in South Korea, it is critical to address not only structural and fire safety but also effective sound insulation. CLT, which can be produced in large panels, is expected to provide excellent airtightness and sound insulation. However, research into the vibration and noise characteristics of CLT slabs is necessary to support the construction of high-quality and noise-efficient timber residential buildings.

Noise transmission in buildings—commonly caused by activities such as footsteps, moving furniture, and other vibrations—remains a major challenge in modern construction. This type of noise, known as impact sound, easily propagates through the structural elements. Recent research has highlighted that the sound insulation performance of CLT depends on factors such as wood species and flooring materials. Hirota *et al.* (2020) investigated the sound insulation properties of CLT slabs made from Japanese larch and fir, reporting that larch performed approximately 4 dB better insulation against rubber ball impacts compared to fir. Additionally, the research demonstrated that the installation of a floating floor over CLT slabs improved sound insulation by 7 to 13 dB.

Similarly, Zhao *et al.* (2021) reported that the impact sound insulation performance improved with increasing concrete topping thickness, with significant improvement observed at 100 mm. Zeitler *et al.* (2014) found that combining rubber cushioning with a concrete topping reduced light impact sound by approximately 21 dB, while Hiramitsu and Hirakawa (2022) observed that concrete toppings were particularly effective against heavy impact sound. Furthermore, finishing materials placed on top of concrete significantly enhanced light impact sound insulation but had a minimal effect on heavy impact sound. These findings underscore the potential for optimizing CLT-based floor systems by selecting appropriate material combinations and configurations.

The structural performance of Korean CLT manufactured from local wood species has been evaluated (Pang and Jeong 2018, 2019; Pang *et al.* 2021), along with its shrinkage and expansion characteristics regarding changes in moisture content (Pang and Jeong 2020). Other studies have explored hybrid CLT using plywood (Choi *et al.* 2015, 2018; Pang *et al.* 2019) and composite slabs that combine CLT and concrete (Quang Mai *et al.* 2018; Pang *et al.* 2022), with an emphasis on structural safety. Recently, Pang *et al.* (2024) investigated the correlation between the vibration and noise performance of CLT slabs, attempting to estimate noise performance based on the vibration characteristics.

Overall, the sound insulation performance of CLT slabs is influenced by the concrete and cushioning materials placed over the CLT panels, which affect the stiffness of the CLT floor. To facilitate the broader adoption of CLT in residential buildings, it is essential to gain a deeper understanding of its sound insulation performance through experimental testing. Therefore, this study investigated the effects of adding precast concrete (PC) and resilient material layers to CLT slabs, particularly focusing on their impact on both sound insulation performance and stiffness.

EXPERIMENTAL

Specimens

To examine the relationship between CLT floor stiffness and improvements in floor impact sound insulation performance, 18 test specimens were prepared using two wood species, six different thicknesses of PC, and an expanded polystyrene (EPS) resilient layer (Won-Hak Lee and Chan-Hoon Haan 2021) (Table 1). The specimen identification (ID) format consisted of three parts: the CLT wood species (first term), the thickness of the PC layer (second term), and the presence or absence of EPS (third term).

Figure 1 depicts the composition of the test specimen, consisting of a CLT panel at the bottom, an EPS layer in the middle, and a PC layer on top. The CLT panels were manufactured from either larch (*Larix kaempferi*) or pine (*Pinus densiflora*) laminae. Each lamina measured 30 mm in thickness, 130 mm in width, and 4,200 mm in length. The laminae were graded according to the KS F 3020 standard using a machine grader (MGFE-251, IIDA Kogyo, Komaki, Japan).

Five layers of laminae were laminated to produce CLT grades C-E10-E8 (larch CLT) and C-E8-E6 (pine CLT), in accordance with the KS F 2081 standard. In this nomenclature, the first letter represents CLT, the second denotes the grade of the outer layers, and the third denotes the grade of the inner layer. Both outer layers used laminae of the same grade, and the three inner layers also used laminae of a uniform grade.

Table 1. Materials and Combinations of Test Specimens

No	Specimen ID	CLT panel		PC panel		EPS	Test slab		
		Species	Dimensions (mm)	Thick-ness (mm)	Area (mm^2)	Thick-ness (mm)	Total thickness (mm)	Area (mm^2)	Mass (kg)
1	L-PC0-N	Larch (*Larix Kaempferi*)	150 (thickness) × 1000 (width) × 4200 (length)	-	1000 (width) × 4200 (length)	-	150	3000 (width) × 4200 (length)	1110
2	L-PC50-E			50		30	230		2591
3	L-PC75-E			75		30	255		3330
4	L-PC100-E			100		30	280		4071
5	L-PC125-E			125		30	305		4811
6	L-PC150-E			150		30	330		5552
7	L-PC210-E			210		30	390		7328
8	L-PC75-N			75		-	225		3330
9	L-PC150-N			150		-	300		5552
10	L-PC210-N			210		-	360		7328
11	P-PC0-N	Pine (*Pinus densiflora*)	150 (thickness) × 1000 (width) × 4200 (length)	-	1000 (width) × 4200 (length)	-	150	3000 (width) × 4200 (length)	900
12	P-PC50-E			50		30	230		2380
13	P-PC75-E			75		30	255		3121
14	P-PC100-E			100		30	280		3861
15	P-PC125-E			125		30	305		4602
16	P-PC150-E			150		30	330		5341
17	P-PC210-E			210		30	390		7118
18	P-PC150-N			150		-	300		5341

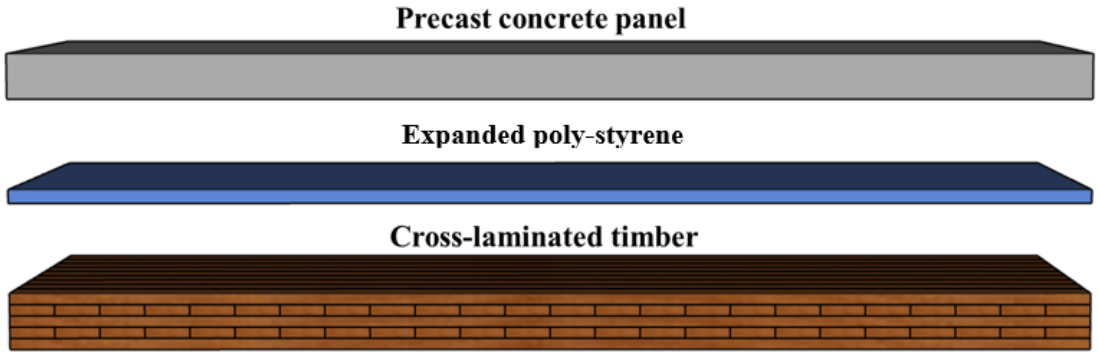

Fig. 1. Composition of materials for test specimens

A phenol–resorcinol–formaldehyde adhesive was used for bonding. It was applied at a level of 200 g/m^2 per layer. The panels were pressured at 1 MPa for 20 h, followed by one week of curing. The mean moisture content of the CLT was 12% ± 2%. The specific gravity of the panels was 0.587 for larch CLT and 0.476 for pine CLT. The overall dimensions of the CLT panel were 150 mm in thickness, 1,000 mm in width, and 4,200 mm in length. For testing, the CLT panels were connected using spline joints to form assemblies measuring 3000 × 4200 mm (Fig. 2). The spline joints were reinforced with self-tapping screws (Ø 6 × 80 mm, HBS model, Rothoblass).

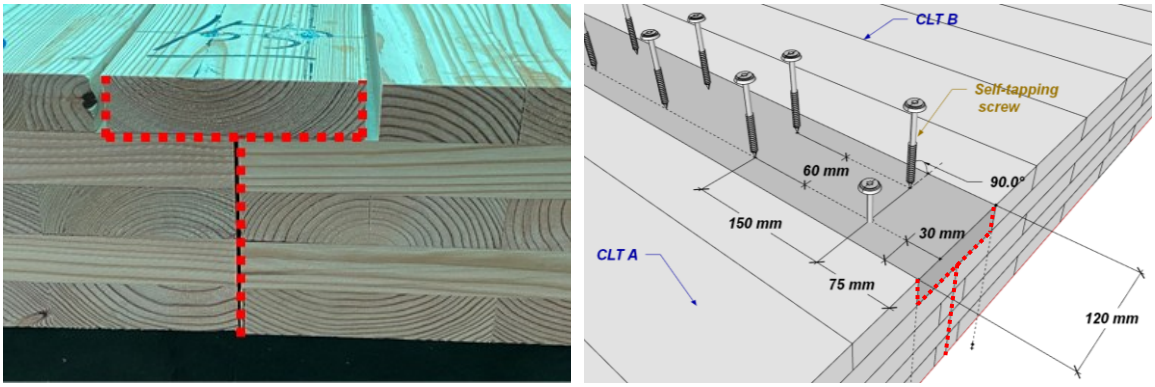

Fig. 2. Joint types used to connect the CLT panels (Pang *et al.* 2024)

Figure 3 depicts the EPS and PC plates used. Flat-type EPS, commonly used in floating floor structures at construction sites, was used as a resilient material, with a thickness of 30 mm. Six types of PC plate were prepared with thicknesses of 50, 75, 100, 125, 150, and 210 mm. Each plate measured 3,000 × 4,200 mm.

Methods

Figure 4 presents the schematic layout of the experimental laboratory. The test slab was installed between an upper reverberation chamber and a lower sound-receiving chamber. In this study, three types of sound insulation performance were evaluated: airborne sound transmission loss (D_w), heavy-weight floor impact sound ($L_{iA,Fmax}$), and light-weight floor impact sound ($L_{nT,w}$). Airborne sound insulation was measured according to KS F ISO 10140-3 2021. Wideband random noise was generated by an omnidirectional loudspeaker (B&K, type 4292L) installed in the upper reverberation chamber and recorded

by five omnidirectional microphones (B&K, type 4189) located in the lower sound-receiving chamber. The recorded signals were analyzed using a multichannel analyzer (B&K, type 3099) to calculate 1/3-octave band sound pressure levels from 50 to 5,000 Hz. From these, the 1/3 octave band sound transmission loss and the single-number rating (D_w) were determined according to KS F 2862 2002. A higher D_w value indicates better airborne sound insulation.

Heavy- and light-weight floor impact sounds were measured following KS F ISO 10140-3 2021 and evaluated as single-number ratings according to KS F ISO 717-2 2020. The microphone-recorded sound pressure levels were divided into 1/3-octave bands within the frequency range of 50 to 630 Hz. Lower $L_{iA,Fmax}$ and $L_{nT,w}$ values represent better sound insulation performance.

a) Expanded polystyrene

b) Precast concrete

Fig. 3. Materials used to improve the sound insulation performance of CLT slabs

All tests were conducted at the Fire Insurers Laboratories of Korea, an internationally certified testing agency specializing in floor impact sound insulation. Each configuration was tested with a single specimen. To ensure reliability despite the one-specimen design, instrument repeatability was verified, and measurements were taken at multiple positions on the slab (five drop positions for heavy impact and multiple microphone positions for airborne sound). This approach provided consistent results across repetitions, supporting the robustness of the dataset.

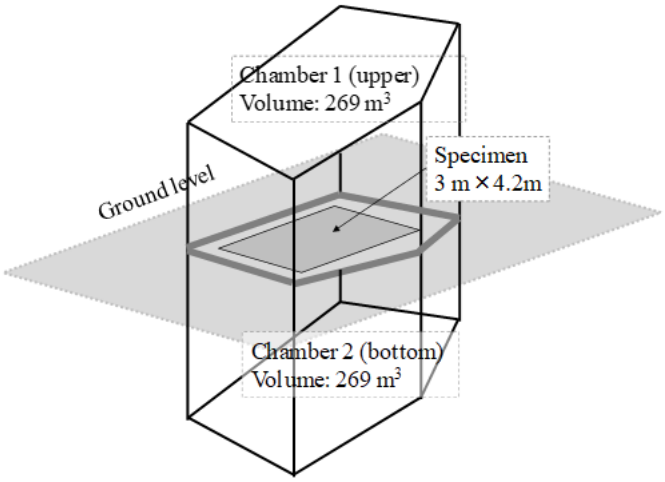

Fig. 4. Schematic diagram of the laboratory for the experiment (Hyo-Jin Lee *et al.* 2023)

Figure 5 illustrates the CLT specimen setup and designated impact source positions (red circle). Heavy-weight floor impact sounds were generated using a standard rubber ball (Rion, YI-01) dropped from a height of 1 m at five points: the center of the slab and four corners positioned 750 mm from the borders of the slab. Each drop was repeated nine times at each specified position. Light-weight floor impact sounds were generated using a tapping machine that simulates hard, repetitive impacts, such as heel tapping. The tapping machine consisted of five 500 g hammers arranged in a line, sequentially dropping at a rate of 10 impacts per second.

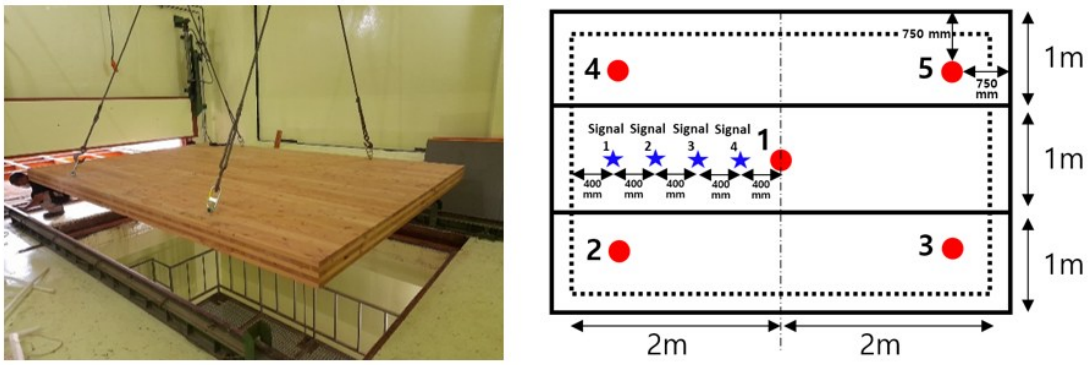

Fig. 5. Installation of CLT specimen and locations for impact source hitting (Pang *et al.* 2024)

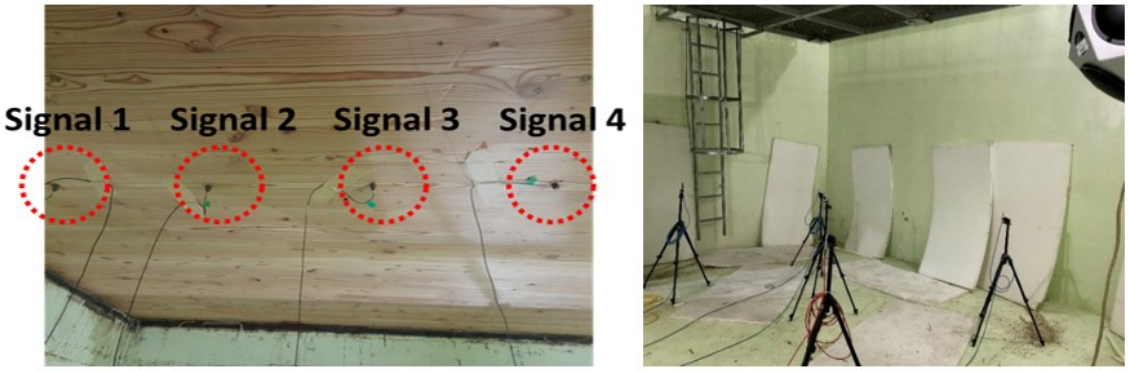

Fig. 6. Installation of accelerometers (left) and microphones (right) (Pang *et al.* 2024)

Figure 6 illustrates the placement of four accelerometers and a microphone beneath the CLT slab. To analyze deflection and the fundamental natural frequency during impact testing, four accelerometers (B&K, type 4527) were mounted at 400 mm intervals under the slab (blue stars in Fig. 4). For sound insulation measurements, five microphones (B&K, type 4189) were installed at a height of 1.2 m within the receiving chamber.

In actual buildings, CLT slabs are commonly supported by beams or by walls along one or more edges. However, the objective of the present experiment was to isolate and evaluate the effects of the concrete and EPS layers on the CLT slab itself. For this reason, as shown in Figs. 5 and 6, the test slabs were installed without any supporting beams or additional vertical supports beneath them. Consequently, in the experimental setup, the CLT slab carried the entire load except for the edges supported by the testing structure.

The slab exhibited multiple natural frequencies corresponding to vibration modes, including bending and torsion. In building design, the first vibration mode is most critical, as low-frequency noise is difficult to isolate, while high-frequency noise can be reduced by floating floor systems or sound-absorbing materials. Accordingly, this study focused on the first vibration mode (largest amplitude), defined as the fundamental natural frequency. The fundamental frequency of each CLT slab was derived by converting the time-domain displacement response into the frequency domain using the Fast Fourier Transform (Xie *et al.* 2020; He *et al.* 2023; Pang *et al.* 2024).

Stiffness of Test Specimens

Three types of stiffness related to slab behavior were evaluated: bending stiffness (*EI)*, dynamic stiffness, and impact stiffness. Bending stiffness represents the resistance of a structural member to deformation under bending. It depends on the material's elastic modulus (*E*) and its geometric properties, particularly the moment of inertia (*I*). The *EI* was calculated using Eq. 1, following Eurocode 5(BS EN 1995-1-1 2004; Wallner-Novak *et al.* 2014),

$$EI = \sum_{i=1}^{n}(E_i \cdot I_i + \gamma_i \cdot E_i \cdot A_i \cdot z_i^2) \quad (1)$$

where EI represents the effective bending stiffness of the test slab (N·mm^2), E_i denotes the modulus of elasticity of i^{th} layer (MPa), I_i indicates the moment of inertia of the i^{th} layer (mm^4), γ_i is the connection efficiency factor of the ith layer ($0 < \gamma \leq 1$), A_i represents the cross-sectional area of the i^{th} layer (mm^2), and z_i denotes the distance between the centroid of the i^{th} layer and the neutral axis of the composite section (mm).

Dynamic stiffness is associated with the slab vibration and indicates its behavior at specific frequencies. It was determined using the mass of the slab and the vibration frequency measured by accelerometers. Assuming simple harmonic motion and approximating the slab system as a single degree-of-freedom vibration system, Eq. 2 describes the relationship among vibration frequency, stiffness, and mass. From this, Eq. 3 was derived as follows,

$$f = \frac{1}{2\pi}\sqrt{\frac{k_{dynamic}}{m}} \quad (2)$$

$$k_{dynamic} = (2\pi f)^2 \cdot \mathrm{m} \quad (3)$$

where f represents the fundamental natural frequency obtained from the acceleration response spectrum (Hz), $k_{dynamic}$ denotes the dynamic stiffness of the CLT slab (N/m), and m indicates the mass of the CLT slab (kg).

The impact stiffness is associated with the slab deflection under out-of-plane loads. It was calculated as the ratio of the applied loads to the maximum deflection, as described in Eq. 4. The applied loads included the impact force from the test ball, the self-weight of the slab, and the weight of the experimenter. The impact force was generated using a hollow silicone rubber ball (185 mm diameter, 30 mm thickness, 2.5 ± 0.2 kg) dropped from a height of 1 m, which produced an impact load of approximately 1,500 N (KS F ISO 10140-3 2021; Yazbec *et al.* 2022; Ha *et al.* 2023; Lee *et al.* 2023).

$$k_{impact} = (W_{impact} + W_{CLT} + W_{experimenter})/\delta_{max} \quad (4)$$

where k_{impact} represents the impact stiffness of the CLT slab (N/m), W_{impact} denotes the impact load from the rubber ball (1,500 N), W_{CLT} indicates the self-weight of the CLT panel (N), $W_{experimenter}$ represents the weight of the experimenter (N), and δ_{max} denotes the maximum slab deflection (mm). Although this quantity is based on static assumptions while the impact load is dynamic, it remains a meaningful indicator in structural analysis, as it is intuitive and indicates a strong correlation with noise levels.

Since it is difficult to measure slab deflection experimentally at all points, the maximum deflection was simulated using the finite element method (FEM) with Midas NFX software (Midas I.T. 2024). The input parameters (material properties) are presented in Table 2. Lamina properties were assumed to be orthotropic.

Table 2. Material Properties for Finite Element Analysis

Material		Density (kg/m^3)	Elasticity[1)] (MPa)	Shear Modulus[2)] (MPa)	Poisson's Ratio[3)]
Larch	E10	587.3	10500 (E_L) 350 (E_T)	656.25 (G_L) 65.625 (G_T)	0.276 (μ_{LT}) 0.352 (μ_{TR}) 0.01 (μ_{RL})
	E8		8500 (E_L) 283.34 (E_T)	531.25 (G_L) 53.125 (G_T)	
Pine	E8	476.0	8500 (E_L) 283.34 (E_T)	531.25 (G_L) 53.125 (G_T)	0.315 (μ_{LT}) 0.308 (μ_{TR}) 0.01 (μ_{RL})
	E6		6500 (E_L) 216.67 (E_T)	406.25 (G_L) 40.625 (G_T)	
Concrete		2350.0	26,702	10,270	0.3
EPS[4)]		15.0	0.086 [5)]	-	-

[1)] E_L: elasticity for longitudinal direction, E_T: elasticity for transverse direction to longitudinal direction
[2)] G_L: shear modulus for longitudinal direction, G_T: shear modulus for transverse direction to longitudinal direction; [3)] μ_{LT}: the Poisson's ratio for tangential deformation due to longitudinal stress, μ_{TR}: the Poisson's ratio for radial deformation due to tangential stress, μ_{RL}: the Poisson's ratio for longitudinal deformation due to radial stress; [4)] Expanded polystyrene; [5)] (Malai and Youwai 2021)

For each grade, elasticity was set to the median value defined in KS F 3020 (Table 2). Transverse elasticity was defined as 1/30 of the longitudinal elasticity, according to the CLT handbook(Innovations 2014). The shear modulus in the longitudinal direction was assumed to be 1/16 of longitudinal elasticity, and the shear modulus in the transverse direction was 1/10 of the longitudinal shear modulus.

Poisson's ratios were based on the Wood Handbook (Ross 2021). In this notation, the first subscript denotes the stress direction and the second represents the lateral deformation direction. For stress applied longitudinally, radial deformation is minimal; therefore, no specific value for μ_{RL} is provided. Following a previous study, μ_{RL} was assumed to be 0.01 in this work (Pang *et al.* 2024).

RESULTS AND DISCUSSION

Effects of the Concrete Layer

Table 3 presents the area density and experimental results (fundamental natural frequency, stiffness, and acoustic performance) of the specimen slabs. The area density was calculated as slab weight divided by area, while the fundamental natural frequency was measured using an accelerometer. The bending stiffness (Eq. 2) was derived from the cross-sectional properties and elastic modulus, dynamic stiffness (Eq. 4) from the fundamental natural frequency and the mass of the slab, and impact stiffness (Eq. 5) from the applied load and measured deflection. Figure 7 depicts the predicted slab deflection under load, with the maximum deflection used to determine impact stiffness.

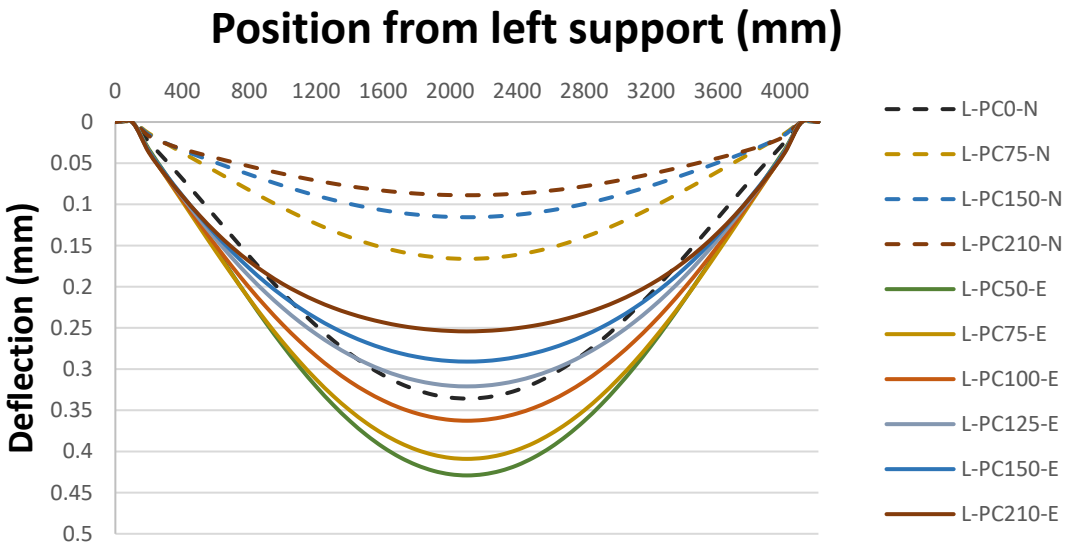

a) Larch CLT-based test slabs

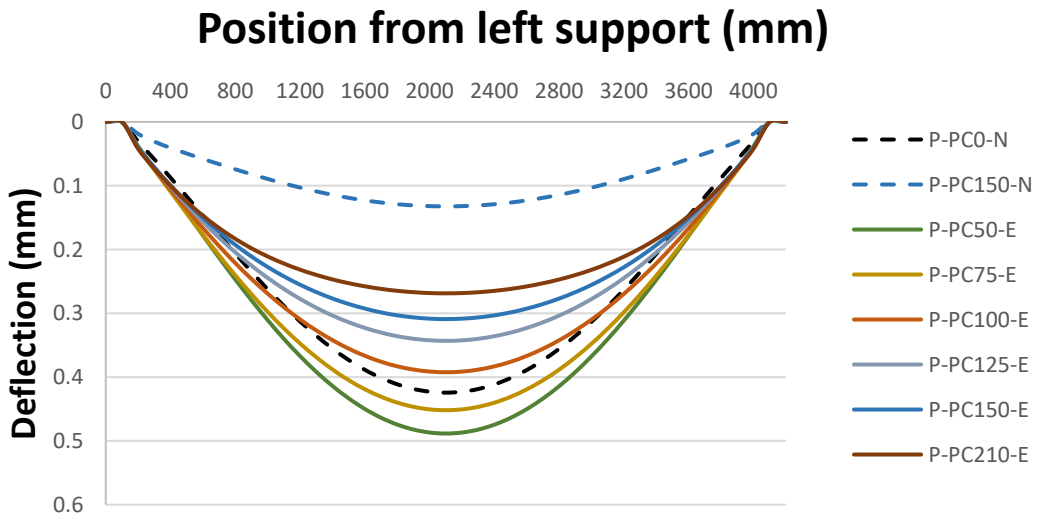

b) Pine CLT-based test slabs

Fig. 7. Deflection of test slabs

Table 3. Experimental Results

No	Specimen ID	Area Density (kg/m^2)	Fundamental Natural Frequency (Hz)	Stiffness (kN/m)			Acoustic Performance[1)]		
				Bending Stiffness ($kN \cdot m^2$)	Dynamic Stiffness (kN/m)	Impact Stiffness (kN/m)	D_w[2)] (dB)	$L_{iA,Fmax}$[3)] (dB)	$L_{nT,w}$[4)] (dB)
1	L-PC0-N	154	20	6,708	17,528	38,758	41	69	78
2	L-PC50-E	361	-	6,709	-	64,273	51	60	58
3	L-PC75-E	463	18	6,711	42,676	85,168	53	61	58
4	L-PC100-E	566	20	6,714	64,376	116,042	53	57	56
5	L-PC125-E	669	16	6,721	48,682	153,716	54	56	54
6	L-PC150-E	772	17	6,730	63,403	194,559	54	56	53
7	L-PC210-E	1,019	17	6,770	83,673	291,141	55	51	49
8	L-PC75-N	463	20	6,711	52,597	209,382	49	61	66
9	L-PC150-N	771	-	6,730	-	489,115	49	57	60
10	L-PC210-N	1,018	24	6,770	166,638	831,860	51	52	59
11	P-PC0-N	125	20	5,368	14,207	25,809	40	72	79
12	P-PC50-E	331	17	5,368	27,220	52,237	52	59	59
13	P-PC75-E	434	17	5,371	35,666	72,521	52	60	58
14	P-PC100-E	537	17	5,378	44,112	102,005	52	58	57
15	P-PC125-E	640	17	5,391	52,557	137,766	52	58	55
16	P-PC150-E	743	18	5,413	68,391	176,434	53	56	53
17	P-PC210-E	989	16	5,475	71,993	267,757	55	52	49
18	P-PC150-N	742	23	5,498	111,545	411,482	46	57	61

(1) From Hyo-Jin Lee *et al.* 2023)
(2) Single-number quantity for airborne sound transmission loss; the higher the value, the better the performance.
(3) Single-number quantity for heavy-weight floor impact sound; the lower the value, the better the performance.
(4) Single-number quantity for light-weight floor impact sound; the lower the value, the better the performance.

The relationship between the PC thickness and the CLT slab stiffness is depicted in Fig. 8, indicating that all types of stiffness increased with greater PC thickness. Bending stiffness, determined from the cross-sectional properties, increased gradually with added concrete (Fig. 8a).

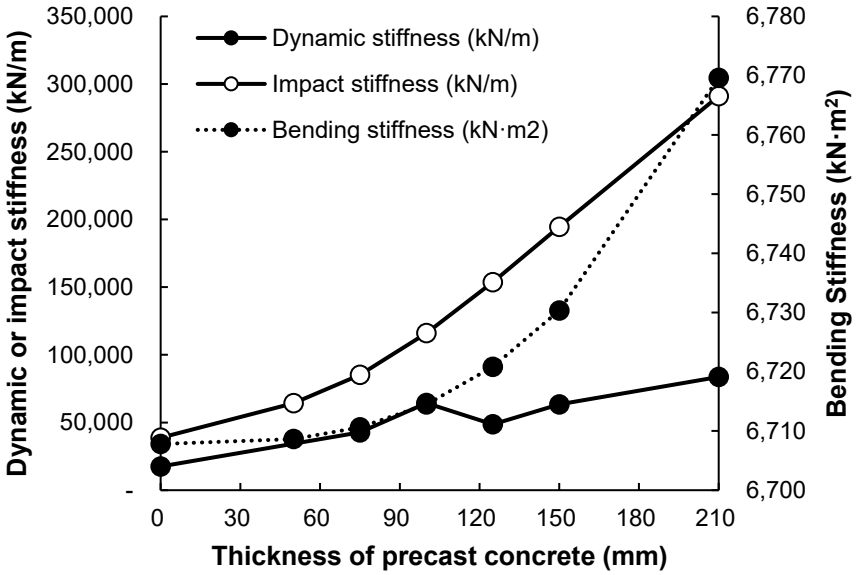

a) Larch CLT-based test slabs

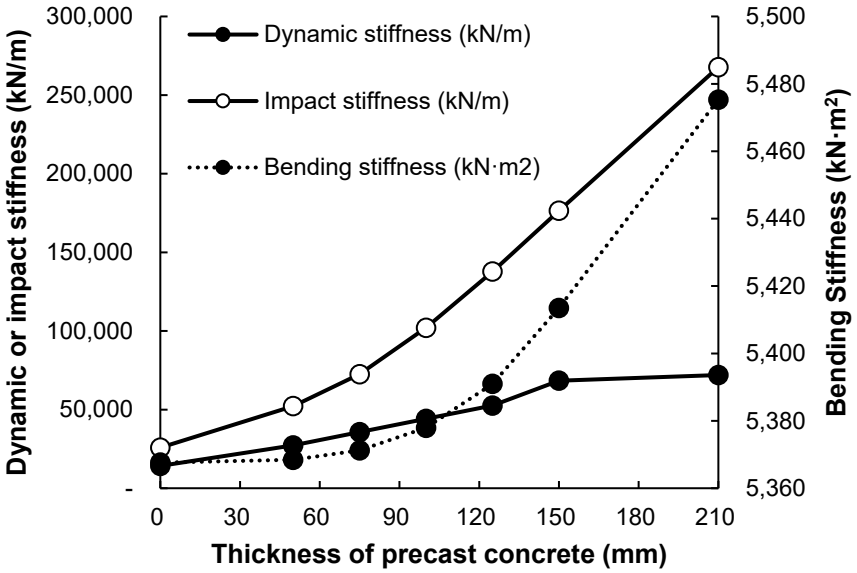

b) Pine CLT-based test slabs

Fig. 8. Effect of precast concrete on the stiffness of test slabs

Conversely, the dynamic stiffness increased with PC thickness but plateaued after 100 mm. This trend was also consistent across both larch and pine CLT specimens (Fig. 8b). Bending and impact stiffness primarily reflect cross-sectional geometry and flexural

modulus, while dynamic stiffness reflects vibration frequency. Because the vibrator was attached to the bottom of the CLT layer, the additional mass and stiffness from the concrete had less influence on CLT frequency. For larch CLT, the effect of added mass on vibration frequency diminished at PC thicknesses above 100 mm, and for pine CLT, above 150 mm. This suggests there is a threshold concrete thickness beyond which further increases have a limited influence on vibration behavior.

Deflection values were greater when EPS was present at the same concrete thickness. This can be attributed to the relatively low stiffness of EPS and variations in the load transfer mechanisms. As a soft material, EPS caused the load from the upper concrete layer to be transferred unevenly, concentrating stress at the center of the CLT. Without EPS, the concrete was bonded directly to the CLT, contributing to flexural resistance. With the implementation of EPS, the indirect connection altered stress transfer, thereby reducing bending stiffness.

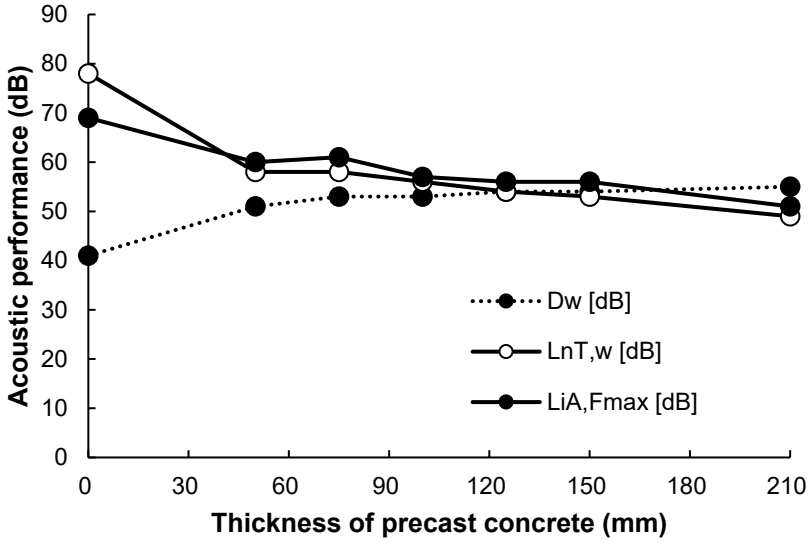

a) Larch CLT-based test slabs

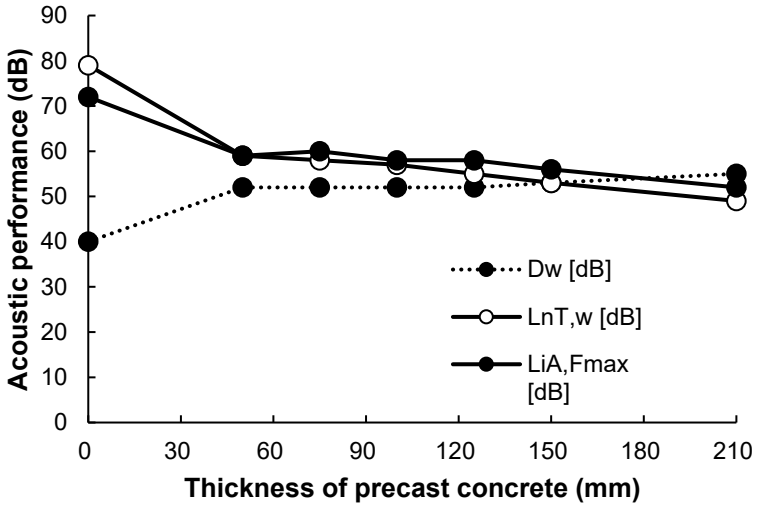

b) Pine CLT-based test slabs

Fig. 9. Effect of precast concrete on the acoustic performance of test slabs

Figure 9 illustrates the relationship between the thickness of PC and acoustic performance. The presence of a concrete layer significantly improved the acoustic performance compared with specimens lacking a layer. Further increases in concrete thickness produced gradual improvements. The sound insulation index (D_w) increased with the thickness of the PC, indicating that thicker concrete enhanced sound insulation (Fig. 9a). In contrast, heavy-weight ($L_{iA,Fmax}$) and light-weight ($L_{nT,w}$) impact noise levels decreased as the PC thickness increased. Similar trends were observed in specimens made from pine CLT (Fig. 9b).

The plateau in performance, even with increasing concrete thickness, may have been influenced by flanking transmission. Previous studies on CLT and timber–concrete floors have also shown that once a slab reaches a certain mass–stiffness level, the acoustic benefit of additional topping mass becomes limited, and further improvements may be masked by non-direct transmission paths such as flanking (Bao *et al.* 2025; Martins *et al.* 2015; Schluessel *et al.* 2014).

Although the experiment was conducted in an internationally certified testing facility using a standardized concrete base, inherent limitations were identified in isolating the transmission behavior of timber slabs, particularly regarding connections and wall-related flanking paths. These findings highlight the need for a testing environment specifically designed for timber slabs to minimize such influences and improve the reliability of future measurements.

Effects of EPS Layer and CLT Species

The stiffness and acoustic performance of slabs with four different PC thicknesses (L-PC75, P-PC150, L-PC150, and L-PC-210) were analyzed with and without the EPS layer. Figure 10(a) depicts the difference in impact stiffness, dynamic stiffness, and bending stiffness depending on the presence of the EPS layer.

As the concrete thickness increased, the overall stiffness of the slab also increased. The slabs with EPS exhibited greater impact stiffness and dynamic stiffness compared to those without EPS, and the difference became more pronounced with thicker concrete layers. The increase in impact stiffness can be attributed to the reduced elasticity of EPS, which altered the way impact loads were transferred to the CLT layer. When EPS was used, loads from the concrete were more centralized rather than evenly distributed, resulting in greater deflection at the center of the CLT slab.

Dynamic stiffness also decreased with the addition of the EPS layer. Acting as a buffer, the EPS layer absorbed part of the vibration energy, lowering the natural frequency (Hz) of the CLT layer. Consequently, despite the added mass of the EPS layer, the slabs with EPS indicated lower dynamic stiffness than those without EPS.

The bending stiffness, which depends on the elastic modulus and cross-sectional area of the material, exhibited only a small difference between the slabs with and without the EPS layer. This is because EPS has an extremely low elastic modulus—approximately 0.0008% of that of structural materials such as concrete and timber (larch and pine)—and its thickness (30 mm) was small compared with that of the CLT and concrete layers.

Figure 10(b) visualizes the acoustic performance of slabs with and without EPS layers. When the EPS layer was installed, $L_{iA,Fmax}$ improved by approximately 5 dB. Meanwhile, increasing concrete thickness by 135 mm (from L-PC75 to L-PC-210) improved $L_{iA,Fmax}$ by approximately 2 dB. Therefore, installing a 30 mm EPS layer was more effective in blocking airborne noise than increasing the concrete thickness.

For impact noise, the light-weight impact noise was reduced by approximately 8

dB with EPS, while the heavy-weight impact noise was reduced by approximately 0.5 dB. This indicates that the EPS layer was highly effective in reducing light-weight impact noise but has minimal impact on heavy-weight impact noise. Overall, the EPS layer was found to be particularly effective in reducing airborne and light-weight impact noise, but less effective against heavy impact noise.

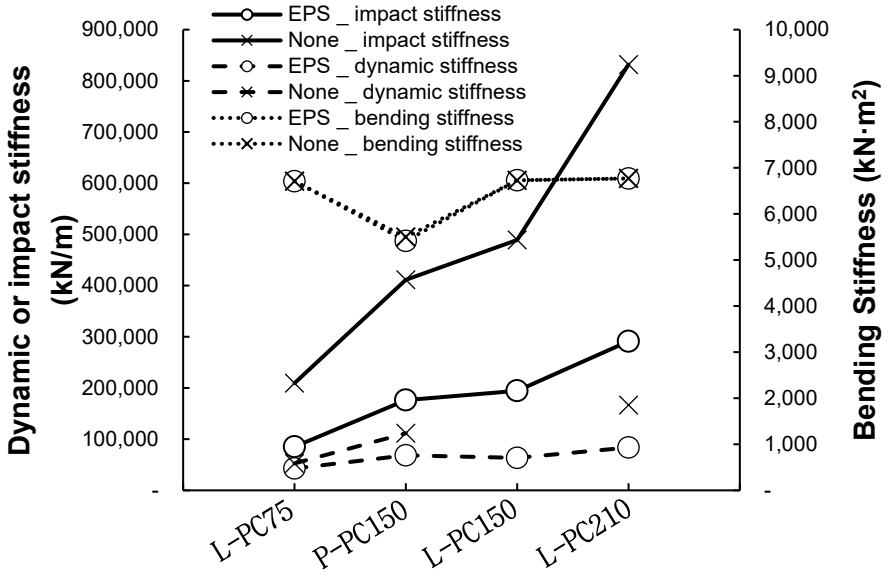

a) Stiffness of test slabs

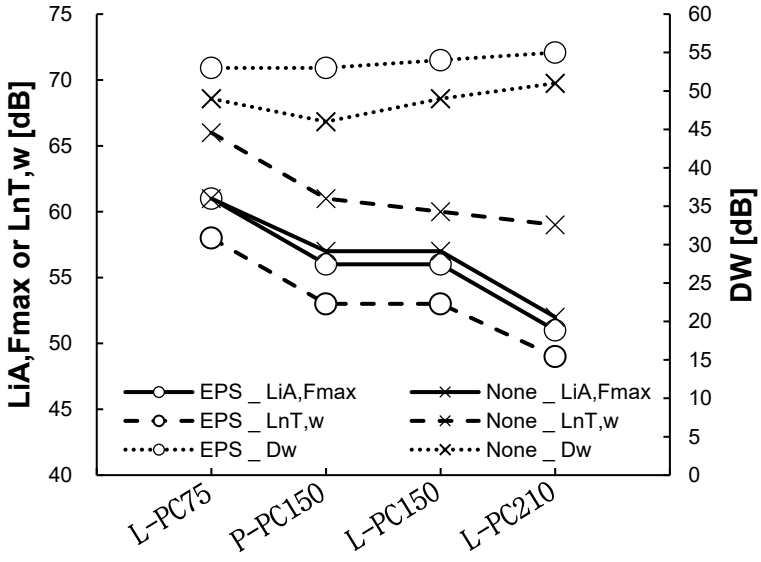

b) Acoustic performance of test slabs

Fig. 10. Effect of EPS layer on the stiffness and acoustic performance of test slabs

Figure 11 compares the stiffness and acoustic performance of slabs made of larch and pine, under the same cross-sectional areas of CLT, concrete, and EPS layers. When larch CLT was used, the bending stiffness was consistently approximately 24.3% higher and the impact stiffness about 19.2% higher than with pine CLT (Figure 11a). This can be

explained by the higher density (approximately 23.4%) and an elastic modulus (approximately 23.5%) of larch compared with pine. In contrast, dynamic stiffness indicated no clear difference between larch and pine CLT, as it reflects overall mass and vibration characteristics. This suggests that the high mass of concrete and the vibration absorption properties of EPS exerted a greater effect on dynamic stiffness than the CLT species.

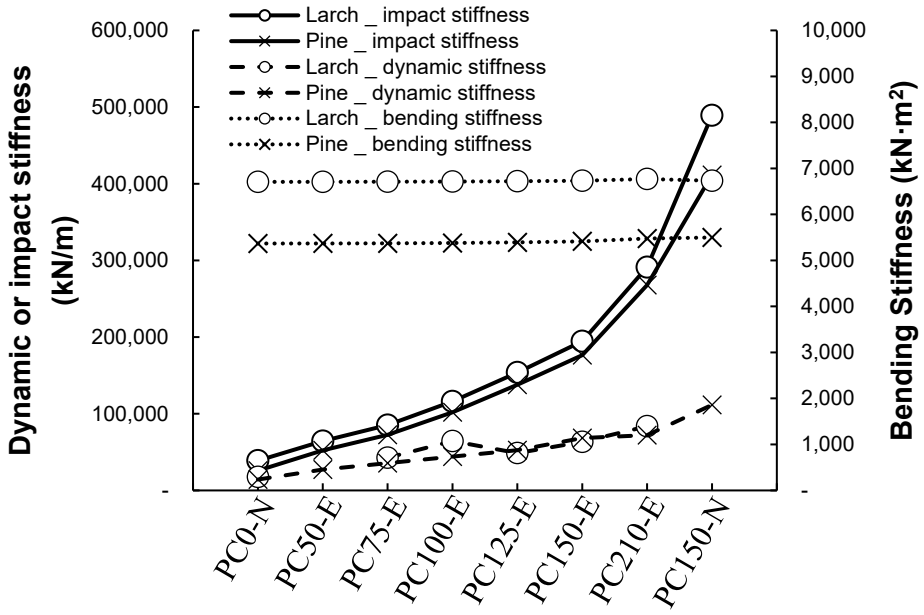

a) Stiffness of test slabs

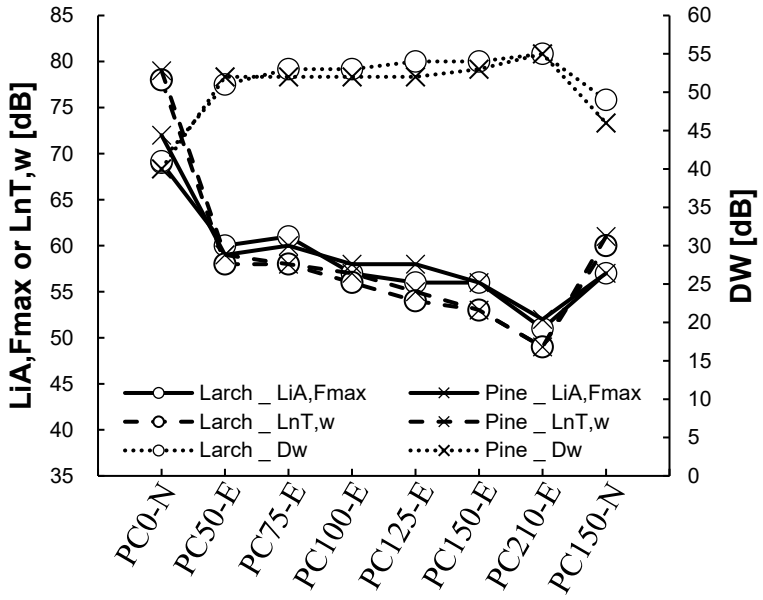

b) Acoustic performance of test slabs

Fig. 11. Effect of CLT species on the stiffness and acoustic performance of test slabs

Figure 11(b) depicts the acoustic performance comparison between larch and pine slabs. The D_w exhibited little difference with CLT species or increasing concrete thickness,

but it improved substantially with EPS. Similarly, $L_{iA,Fmax}$ and $L_{nT,w}$ varied little with CLT species but decreased significantly with EPS, and continued to decrease gradually with thicker concrete. Therefore, these results indicate that the effects of CLT species on acoustic performance were minimal compared with the dominant influences of concrete and EPS.

Relationship between Stiffness and Acoustic Performance

Figure 12 depicts the relationship between stiffness and acoustic performance of test slabs with the EPS layer.

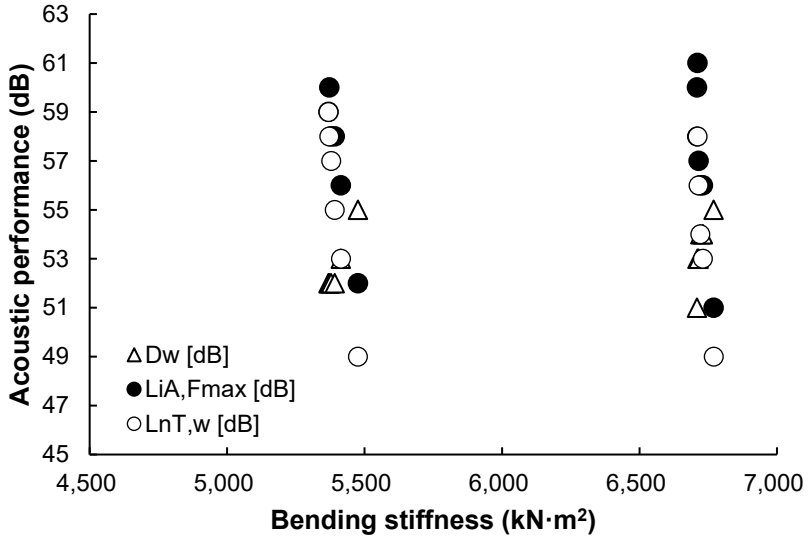

a) Bending stiffness on acoustic performance

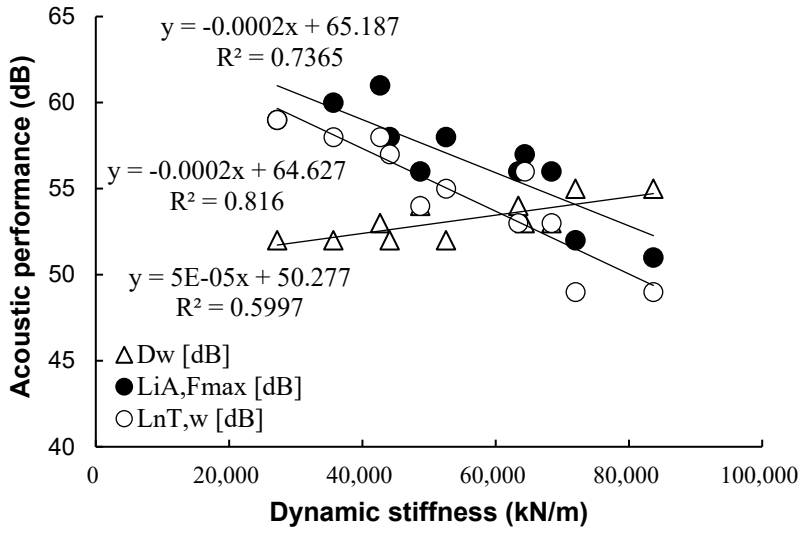

b) Dynamic stiffness on acoustic performance

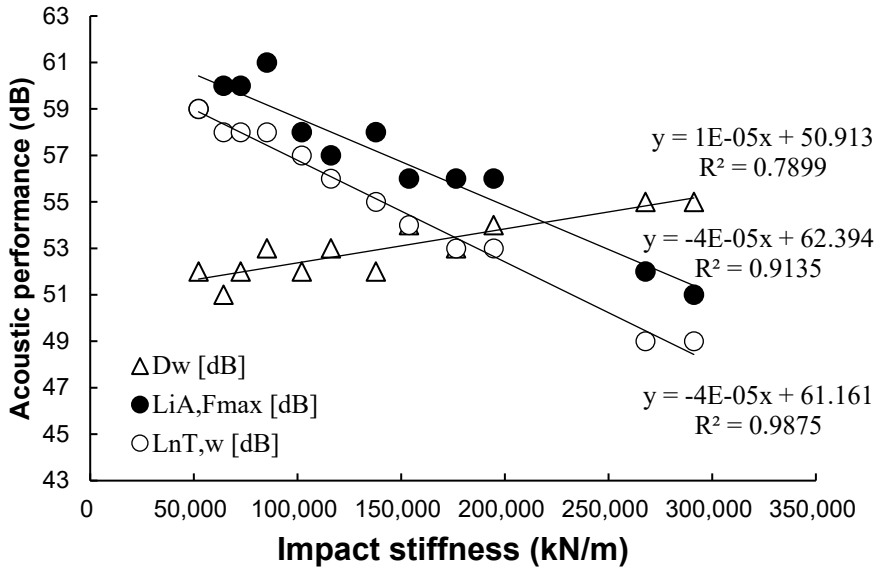

c) Impact stiffness on acoustic performance

Fig. 12. Relationship between stiffness and acoustic performance

The bending stiffness was influenced more by the elasticity of CLT than by the concrete or EPS layers. Consequently, when larch CLT was used, the bending stiffness was 24.3% higher than when pine CLT was used. The bending stiffness of specimens with larch CLT was concentrated around 6700 kN·m², while those with pine CLT were concentrated around 5400 kN·m² (Fig. 12a). Because of this large difference between CLT species, a non-significant correlation was found between bending stiffness and acoustic performance.

Figure 12(b) indicates the relationship between dynamic stiffness and acoustic performance of test slabs. The dynamic stiffness was distributed over a wide range, indicating a different pattern from the relationship between bending stiffness and acoustic performance. Since dynamic stiffness was affected by the mass and frequency of the slab, increases in CLT density and concrete thickness improved dynamic stiffness. Consequently, both $L_{iA,Fmax}$ and $L_{nT,w}$ exhibited negative correlations with dynamic stiffness, with R^2 values of 0.7365 and 0.816, respectively. In contrast, D_w exhibited a weaker positive relationship with dynamic stiffness ($R^2 = 0.5997$). These findings indicate that dynamic stiffness was more closely related to impact noise than to airborne noise.

Figure 12(c) depicts the relationship between impact stiffness and acoustic performance. The trend was similar to that of dynamic stiffness, but impact stiffness indicated an even higher correlation (R^2 value) with acoustic performance. Impact load depends on both the applied load and the maximum deflection of the slab, where the mass of all materials contributed to the load, and the elastic modulus affected deflection. This explains why the physical and mechanical properties of the CLT species were more strongly reflected in impact stiffness than in dynamic stiffness.

Previous researchers have used area density as a predictor of acoustic performance. Figure 13 depicts the correlation between area density and acoustic performance of test slabs. While area density exhibited a strong correlation, the results above demonstrate that impact stiffness has an even stronger relationship with acoustic performance.

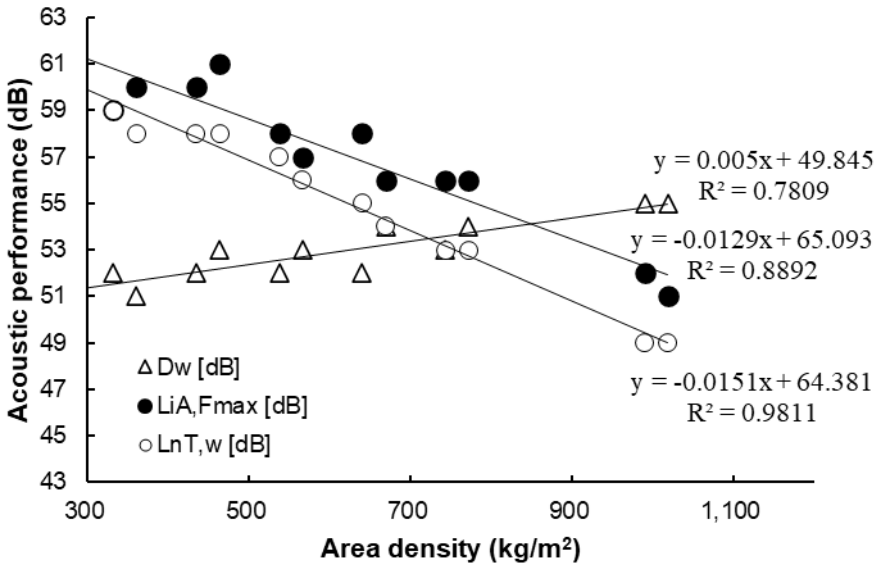

Fig. 13. Relationship between area density and acoustic performance

Overall, this study contributes to improving the acoustic performance of CLT structures in timber buildings. The findings can guide the design and material selection of CLT structures aimed at reducing floor impact sound in timber construction.

CONCLUSIONS

1. The expanded polystyrene (EPS) layer significantly enhanced light impact noise (by 8 dB) and airborne sound insulation (by 5 dB), but it had only a minor effect on heavy impact noise (0.5 dB). Notably, the EPS layer increased D_w by approximately 5 dB, which is more effective than increasing the PC thickness by 135 mm (from L-PC75 to L-PC210), which improved D_w by approximately 2 dB.
2. Increasing the thickness of the precast concrete (PC) layer improved the stiffness and sound insulation performance of cross laminated timber (CLT) slabs. However, improvements in dynamic stiffness slowed once the concrete thickness exceeded 100 mm for larch CLT and 150 mm for pine CLT.
3. The bending stiffness of larch CLT slabs was consistently about 24.3% higher than that of pine CLT slabs (concentrated around 6700 kN·m² for larch and around 5400 kN·m² for pine CLT). Similarly, the impact stiffness of larch CLT slabs was about 19.2% higher than that of pine CLT slabs, due to the higher density and elastic modulus of larch.
4. The impact stiffness indicated a stronger correlation with acoustic performance than area density, which has traditionally been used as a predictor. This suggests that impact stiffness is a more effective indicator for predicting the acoustic performance of slabs.

ACKNOWLEDGEMENTS

This research was supported by a Research Project (FP0200-2022-01-2025) through the National Institute of Forest Science (NIFoS), Korea.

Competing Interests

The authors declare they have no competing interest.

Authors' Contributions

Sung-Jun Pang analyzed the test results and drafted the manuscript. Hyo-Jin Lee and Yeon-Su Ha designed the experimental test procedures and analyzed the acoustic performance. Chul-Ki Kim provided the mechanical properties of CLT. Ji-Ho Chang and Ho-Jeong Cho revised the manuscript, including figures and tables. Sang-Joon Lee managed the research project and approved the final manuscript.

REFERENCES CITED

Arehart, J. H., Hart, J., Pomponi, F., and D'Amico, B. (2021). "Carbon sequestration and storage in the built environment," *Sustainable Production and Consumption* 27, 1047-1063. https://doi.org/10.1016/j.spc.2021.02.028

Bao, Y., Yue, K., Dai, C., Wu, P., Lu, W., Zhao, H., and Li, Q. (2025). "Investigating impact sound insulation in cross-laminated timber (CLT)-concrete composite floors with embedded mechanical fastening: Experimental analysis and statistical energy analysis," *Journal of Building Engineering* 111, article 113216. https://doi.org/10.1016/j.jobe.2025.11321

Berger, F., Gauvin, F., and Brouwers, H. J. H. (2020). "The recycling potential of wood waste into wood-wool/cement composite," *Construction and Building Materials* 260, article 119786. https://doi.org/10.1016/j.conbuildmat.2020.119786

Bjånesøy, S., Kinnunen, A., Einarsdóttir, H., and Heinonen, J. (2023). "Carbon storage in the built environment: A review," *Environmental Research: Infrastructure and Sustainability* 3(4), article 042003. https://doi.org/10.1088/2634-4505/ad139f

BS EN 1995-1-1 (2004). "Eurocode 5: Design of timber structures - Part 1-1: General - Common rules and rules for buildings," European Committee for Standardization, Brussels, Belgium.

Choi, C., Kojima, E., Kim, K.-J., Yamasaki, M., Sasaki, Y., and Kang, S.-G. (2018). "Analysis of mechanical properties of cross-laminated timber (CLT) with plywood using Korean larch," *BioResources* 13(2), 2715-2726. https://doi.org/10.15376/biores.13.2.2715-2726

Choi, C., Yuk, C.-R., Yoo, J.-C., Park, J.-Y., Lee, C.-G., and Kang, S.-G. (2015). "Physical and mechanical properties of cross laminated timber using plywood as core layer," *Journal of the Korean Wood Science and Technology* 43(1), 86-95. https://doi.org/10.5658/WOOD.2015.43.1.86

Gibson, B., Nguyen, T., Sinaie, S., Heath, D., and Ngo, T. (2022). "The low frequency structure-borne sound problem in multi-storey timber buildings and potential of acoustic metamaterials: A review," *Building and Environment* 224, article 109531. https://doi.org/10.1016/j.buildenv.2022.109531

Ha, Y.-S., Lee, H.-J., Lee, S.-J., Shin, J.-A., and Song, D.-B. (2023). "A study on floor

impact sound insulation performance of cross-laminated timber (CLT): Focused on joint types, species and thicknesses," *Journal of the Korean Wood Science and Technology* 51(5), 419-430. https://doi.org/10.5658/WOOD.2023.51.5.419

Harte, A. M. (2017). "Mass timber – The emergence of a modern construction material," *Journal of Structural Integrity and Maintenance* 2(3), 121-132. https://doi.org/10.1080/24705314.2017.1354156

He, Y., Liu, Y., Wu, M., Fu, J., and He, Y. (2023). "Amplitude dependence of natural frequency and damping ratio for 5 supertall buildings with moderate-to-strong typhoon-induced vibrations," *Journal of Building Engineering* 78, article 107589. https://doi.org/10.1016/j.jobe.2023.107589

Hiramitsu, A., and Hirakawa, S. (2022). "Effect of concrete topping on floor impact sound insulation performance of CLT floor," in: *Internoise 2022 - 51st International Congress and Exposition on Noise Control Engineering*, Glasgow, Scotland. https://doi.org/10.3397/in_2022_0595

Hirota, T., Iizumi, G., Nobuo, M., and Miyauchi, J. (2020). "Floor impact sound insulation performance of floating floor method using CLT floor panel of small board made by Hokkaido," *Proc. AIJ Hokkaido Architectural Research Conference* 93, 173-176.

Eom, H. J., Kong, S., and Park, J. (2019). "Based on structural type and fire resistance certification Type A study on the analysis of high-rise wooden architecture," *Journal of Korea Institute of Spatial Design* 14(6), 177-186. https://doi.org/10.35216/kisd.2019.14.6.177

Innovations, F. (2014). *CLT Handbook*, *Igarss 2014*.

Kang, C.-W., Jang, S.-S., Hashitsume, K., and Kolya, H. (2023). "Estimation of impact sound reduction by wood flooring installation in a wooden building in Korea," *Journal of Building Engineering* 64, article 105708. https://doi.org/10.1016/j.jobe.2022.105708

Kromoser, B., Reichenbach, S., Hellmayr, R., Myna, R., and Wimmer, R. (2022). "Circular economy in wood construction – Additive manufacturing of fully recyclable walls made from renewables: Proof of concept and preliminary data," *Construction and Building Materials* 344, article 128219. https://doi.org/10.1016/j.conbuildmat.2022.128219

KS F 2081 (2021). "Cross laminated timber," Korean Standards Association, Seoul, Korea.

KS F 2862 (2002). "Method of evaluating the air transmitting sound insulation performance of building and building members," Korean Standards Association, Seoul, Korea.

KS F ISO 717-2 (2020). "Acoustics — Rating of sound insulation in buildings and of building elements — Part 2: Impact sound insulation," Korean Standards Association, Seoul, Korea.

KS F ISO 10140-3 (2021). "Acoustics—Laboratory Measurement of Sound Insulation of Building Element—Part 3: Measurement of Impact Sound Insulation," Korean Standards Association, Seoul, Korea.

Lee, H.-J., Ha, Y.-S., and Lee, S.-J. (2023). "Evaluation of floor impact sound and airborne sound insulation performance of cross laminated timber slabs and their toppings," *The Journal of the Acoustical Society of Korea* 42(6), 572-583.

Lee, W-H., and Haan, C.- H. (2021). "Characteristics of the floor impact sound by water to binder ratio of mortar," *The Journal of the Acoustical Society of Korea* 40(6),

671-677.
Lippke, B., Wilson, J., Meil, J., and Taylor, A. (2010). "Characterizing the importance of carbon stored in wood products," *Wood and Fiber Science* 42(SUPPL. 1).
Loss, C., Piazza, M., and Zandonini, R. (2016a). "Connections for steel–timber hybrid prefabricated buildings. Part II: Innovative modular structures," *Construction and Building Materials* 122, 796-808. https://doi.org/10.1016/j.conbuildmat.2015.12.001
Loss, C., Piazza, M., and Zandonini, R. (2016b). "Connections for steel–timber hybrid prefabricated buildings. Part I: Experimental tests," *Construction and Building Materials* 122, 781-795. https://doi.org/10.1016/j.conbuildmat.2015.12.002
Malai, A., and Youwai, S. (2021). "Stiffness of expanded polystyrene foam for different stress states," *International Journal of Geosynthetics and Ground Engineering* 7(4), article 80. https://doi.org/10.1007/s40891-021-00321-7
Martins, C., Santos, P., Almeida, P., Godinho, L., and Dias, A. (2015). "Acoustic performance of timber and timber-concrete floors," *Construction and Building Materials*, 101. https://doi.org/10.1016/j.conbuildmat.2015.10.14
Midas (2024). *User's Manual of Midas NFX*, MIDAS Information Technology Co., Ltd., Korea.
Ministry of Land, Infrastructure and Transport. (2022). "Recognition and management standards for multifamily floor sound insulation structures," https://www.law.go.kr/LSW/admRulLsInfoP.do?admRulSeq=2100000217329
Pajchrowski, G., Noskowiak, A., Lewandowska, A., and Strykowski, W. (2014). "Wood as a building material in the light of environmental assessment of full life cycle of four buildings," *Construction and Building Materials* 52, 428-436. https://doi.org/10.1016/j.conbuildmat.2013.11.066
Pang, S. J., Ahn, K. S., Jeong, S. man, Lee, G. C., Kim, H. S., and Oh, J. K. (2022). "Prediction of bending performance for a separable CLT-concrete composite slab connected by notch connectors," *Journal of Building Engineering* 49, article 103900. https://doi.org/10.1016/j.jobe.2021.103900
Pang, S. J., and Jeong, G. Y. (2019). "Effects of combinations of lamina grade and thickness, and span-to-depth ratios on bending properties of cross-laminated timber (CLT) floor," *Construction and Building Materials* 222, 142-151. https://doi.org/10.1016/j.conbuildmat.2019.06.012
Pang, S. J., and Jeong, G. Y. (2020). "Swelling and shrinkage behaviors of cross-laminated timber made of different species with various lamina thickness and combinations," *Construction and Building Materials* 240, article 117924. https://doi.org/10.1016/J.CONBUILDMAT.2019.117924
Pang, S.-J., and Jeong, G. Y. (2018). "Load sharing and weakest lamina effects on the compressive resistance of cross-laminated timber under in-plane loading," *Journal of Wood Science* 64(5), 538-550. https://doi.org/10.1007/s10086-018-1741-9
Pang, S.-J., Lee, H.-J., Ha, Y.-S., Kim, C.-K., Cho, H.-J., and Lee, S.-J. (2024). "Fundamental natural frequency and floor impact sound insulation performance of CLT slabs based on wood species and panel connections: An experimental study," *BioResources* 20(1), 100-120. https://doi.org/10.15376/biores.20.1.100-120
Pang, S.-J., Lee, H.-J., Yang, S. M., Kang, S. G., and Oh, J.-K. (2019). "Moment and shear capacity of Ply-lam composed with plywood and structural timber under out-of-plane bending," *Journal of Wood Science* 65(1), 68. https://doi.org/10.1186/s10086-019-1847-8

Pang, S.-J., Shim, K.-B., and Kim, K.-H. (2021). "Effects of knot area ratio on the bending properties of cross-laminated timber made from Korean pine," *Wood Science Technology* 55(2), 489-503. https://doi.org/10.1007/s00226-020-01255-5

Penman, J., Gytarsky, M., Hiraishi, T., Irving, W., and Krug, T. (2006). *2006 IPCC - Guidelines for National Greenhouse Gas Inventories*, *Directrices para los inventarios nacionales GEI*.

Quang Mai, K., Park, A., Nguyen, K. T., and Lee, K. (2018). "Full-scale static and dynamic experiments of hybrid CLT–concrete composite floor," *Construction and Building Materials* 170, 55-65. https://doi.org/10.1016/j.conbuildmat.2018.03.042

Ross, R. (2021). *Wood Handbook: Wood as an Engineering Material*, U.S. Department of Agriculture, Forest Products Laboratory, Madison, WI, USA.

Schluessel, M., Shrestha, R., and Crews, K. (2014). "Acoustic performance of timber and timber-concrete composite floors.", *WCTE 2014-World Conference on Timber Engineering, Proceedings.* World Conference on Timber Engineering (WCTE).

Wallner-Novak, M., Koppelhuber, J., and Pock, K. (2014). "Cross-laminated timber structural design—basic design and engineering principles according to Eurocode," ProHolz, Innsbruck, Austria.

Xie, Z., Hu, X., Du, H., and Zhang, X. (2020). "Vibration behavior of timber-concrete composite floors under human-induced excitation," *Journal of Building Engineering* 32, 101744. https://doi.org/10.1016/j.jobe.2020.101744

Yazbec, E., Specht, M., Kiefer, D., Harrington, R., Marchi, J., Girdhar, S., DeClerk, Dr. J., and Barnard, Dr. A. (2022). "Investigation of an alternative force input method for impact sound rating," *INTER-NOISE and NOISE-CON Congress and Conference Proceedings* 264(1), 198-208. https://doi.org/10.3397/NC-2022-714

Zeitler, B., Schoenwald, S., and Sabourin, I. (2014). "Direct impact sound insulation of cross laminate," in: *International Congress on Noise Control Engineering*, Melbourne, Australia. https://doi.org.10.13140/2.1.3929.5685

Zhao, Z., Zhou, J., and Li, G. (2021). "Efficiency of floating concrete toppings on mass timber floors for impact sound insulation," in: *World Conference on Timber Engineering 2021*, Santiago, Chile.

Article submitted: October 15, 2025; Peer review completed: November 22, 2025;
Revised version received: November 25, 2025; Accepted: November 30, 2025;
Published: January 20, 2026,
DOI: 10.15376/biores.21.1.2101-2122